

ic sites are involved. However, these still remain open conjectures.

A brief description of a useful graphical technique to perform the calculations might also be of interest. The equation for total concentration can be rearranged to give:

$$x = \frac{w}{p} \left(\frac{C_T}{w} - C \right) \\ = f(C), \text{ binding isotherm} \quad (\text{Eq. A2})$$

This expression is a straight line; if it is plotted on the same graph as $x = x(C)$, the intersection provides the desired value of free concentration corresponding to a (given) total concentration of drug present (see Fig. A1). Shen and Gibaldi used an iterative computer routine to determine the solution of the nonlinear algebraic equation, but the simple graphical technique often provides answers of adequate accuracy, or they could be used as starting values for an iterative computer solution.

To conclude, the questions raised by Shen and Gibaldi concerning the effective protein concentration concept are valid and were the basis of our choice of the term "effective." We did not feel that the data we used (1954 vintage) were sufficiently precise, nor was there a wide enough range of information, to be worth more detailed analysis. We had hoped that more extensive and detailed investigations would be done to test the conjectures. It does seem, however, that good simulations and predictions of tissue drug levels are possible, both from our own work and that of others during

the intervening several years. As discussed by Shen and Gibaldi, the alternate method of utilizing a tissue-plasma distribution ratio, $R(c)$ varying with concentration for nonlinear binding and estimated from *in vivo* data, is probably the best approach in light of our present knowledge of binding.

However, this approach has limitations: (a) a fairly large amount of *in vivo* biopsy data is required, since predictions from *in vitro* binding isotherm data are presumably not used; and (b) interesting effects, such as binding saturation and/or competitive binding of two drugs, cannot be predicted. Therefore, it is felt that the effective protein concentration concept has valuable and unique capabilities for pharmacokinetic simulations, and it is hoped that further development of it, along with fundamental binding studies with physiological protein concentrations, will lead to a more firm quantitative basis for handling drug binding.

Kenneth B. Bischoff

School of Chemical Engineering
Cornell University
Ithaca, N.Y.

Robert L. Dedrick

Biomedical Engineering and
Instrumentation Branch
National Institutes of Health
Bethesda, Md.

Mechanistic Studies on Effect of Cholate Concentration on Cholesterol Uptake by Isolated Rabbit Intestine

ANWAR B. BIKHAZI** and JEAN JACQUES HAJJAR †

Abstract □ A novel apparatus was designed to measure the uptake of cholesterol by mounted and isolated segments of rabbit intestine. The system maintained constant hydrodynamic conditions at the exposed mucosal surfaces. Cholesterol uptake was studied in a series of Ringer's solutions containing different cholate concentrations. The data indicated a substantial effect of cholate on cholesterol transport. A simple semi-infinite sink model in conjunction with theoretical equations on a first-order transport process was proposed. First-order uptake rate constants for the early experimental data points were calculated for the various cholesterol-cholate systems. At 4.64 mM cholate, there was approximately a 190 times increase in the relative initial uptake rate compared to the 0 mM cholate level. Above the CMC of cholate, there was a decrease in the cholesterol uptake. The diffusion coefficients of cholesterol in the various cholate media varied between 3.6 and 13.0 ×

10⁻⁶ cm²/sec, which were in the range of 4.0 × 10⁻⁶ cm²/sec calculated by the Stokes-Einstein approximation. The calculated permeability coefficients of cholesterol, below and above the CMC of cholate, were on the order of 0.8–9.0 × 10⁻² cm/sec.

Keyphrases □ Cholate—effect on cholesterol uptake, isolated rabbit intestine, new apparatus described and tested, CMC and permeability coefficients □ Cholesterol—effect of cholate concentration on uptake by isolated rabbit intestine, new apparatus described and tested, CMC and permeability coefficients □ Transport rates—effect of cholate concentration on cholesterol uptake by isolated rabbit intestine, new apparatus described and tested □ Permeability—effect of cholate concentration on cholesterol uptake by isolated rabbit intestine, new apparatus described and tested

The mechanism of cholesterol transport across the intestine has been under considerable debate for the past few years. Several investigators have emphasized the role that bile salts play in the enhancement of cholesterol absorption (1, 2). Their observations led to the prevalent view that micellar solubilization is essential for cholesterol absorption.

Sylvén and Borgström (3) proposed a possible model for cholesterol transport through the intestinal barrier. This model was later expanded (4) at a

slightly higher mechanistic level. These models, however, need stronger *in vivo* experimental support, particularly with respect to the mechanism of cholesterol transport at submicellar as well as micellar concentration levels of bile salts. Hofmann (5) estimated the critical micelle concentration (CMC) of bile salts to be in the range of 2–3 mM. Rough calculations, considering the bile salt concentration in gallbladder bile, the volume of bile secreted per meal, and the dilution of bile salts in the intestinal volume and con-

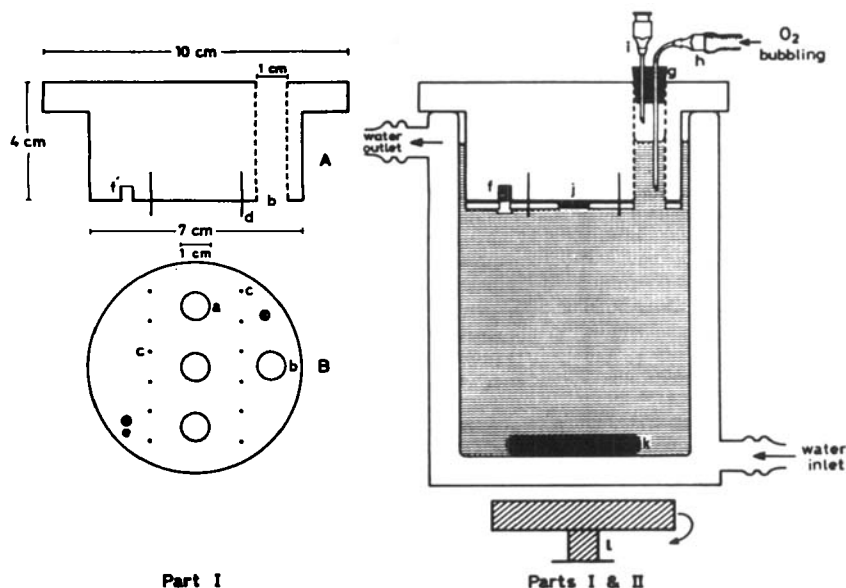


Figure 1—Uptake apparatus. Part I consists of components A and B to be attached together with screws *f* through openings *e* and *f'*. Openings *a* appear only in component B to expose 1-cm diameter of intestine as shown in *j*. Needles *d* penetrate through openings *c* to hold tight the intestinal pieces. Hypodermic needles *h* and *i* are the inlet and outlet of oxygen gas bubbles attached through cork *g* on top of sampling opening *b*; *k* is a Teflon-coated magnetic bar, and *l* is a magnetized shaft of the synchronous motor.

tents, resulted in numbers indicating that intestinal fluids contain bile salt micelles (the concentration of bile salts in the intestinal content is around 2–3 mM).

The present work is an attempt to establish quantitatively a means of measuring cholesterol uptake by the intestine.

EXPERIMENTAL

Treatment of Animals and Description of Apparatus—Mongrel rabbits were utilized and sacrificed by intravenous injection of sodium pentobarbital (6). The abdomen was opened rapidly and segments of the ileum were resected out, slit open along the mesenteric border, and washed free of intestinal contents with cold Ringer's solution, pH 6.90 (140 mM NaCl, 1.2 mM CaCl₂, and 1.2 mM MgCl₂). Three segments were mounted on component A of Part I of the apparatus (Fig. 1). Then component B of Part I immediately was gently placed over component A and firmly attached to it using two screws. This step resulted in exposing three 1-cm diameter portions of mucosal surfaces. Part I of the apparatus then was submerged in a constant-temperature (37 ± 0.1°) water-jacketed beaker which contained a pre-equilibrated Ringer's solution with a known amount of cholesterol-4-¹⁴C (10⁻⁹ g/ml)¹ and/or cholic-³H acid (7 × 10⁻⁹ g/ml)² and the desired concentration of sodium cholate³ (biochemical purity). Into this solution, 95% O₂-5% CO₂ was gently bubbled through opening *b* of Part I of the apparatus with the help of a hypodermic needle attached through a Teflon tube to an oxygen tank. The bubbling was very cautiously controlled so as not to disturb the stirring of the system and thereby alter the diffusional mechanisms at the surfaces of the membranes. The Ringer's solution in the apparatus was constantly stirred before and during the experiments by utilizing a Teflon-coated magnetic bar rotating at 120 rpm with a synchronous constant-speed motor⁴ placed beneath the beaker. This synchronous stirring process assured constant hydrodynamic conditions at the exposed surfaces of the intestine.

Sampling and Assay of Samples—To measure the rate of disappearance of cholesterol from the system, 1-ml samples were taken through opening *b* of Part I at different time intervals. These samples were assayed for cholesterol-4-¹⁴C and/or cholic-³H acid in a three-channel liquid scintillation spectrometer⁵ using Bray's solution (7). Control experiments were done to measure the adsorption of cholesterol on glass and on Leucite in the absence of

the intestinal segments. The amount of solute adsorbed in the presence of Ringer's solution was found to be negligible for a 1-hr period.

Determination of Cholate CMC in Ringer's Solution—The CMC of sodium cholate was determined in Ringer's solution employing the volume-per-drop method. Sodium cholate concentrations ranging from 0 to 23.2 mM were freshly prepared in Ringer's solution. A Teflon-tipped buret was vertically assembled. The level of each cholate solution in the buret was adjusted to be the same at the beginning of every count. The number of droplets delivered from the buret per 5-ml volume was counted for each surfactant solution.

Measurement of Diffusion Layer Thickness—The method of Howard (8) was used in measuring the diffusion layer thickness along the intestinal mucosa at a 120-rpm stirring rate in the aqueous bulk phase. A 0.005% *p*-nitrotoluene stock solution in Ringer's solution was prepared. The procedure described under *Treatment of Animals and Description of Apparatus* was employed, except that the *p*-nitrotoluene stock solution was put in the water-jacketed beaker replacing the cholesterol-cholate solution. Two-milliliter samples were taken at different time intervals for 90 min. The samples were then diluted with 10 ml of water and read against the proper blank in a spectrophotometer⁶ at λ_{max} 285 nm. The concentrations of the samples were calculated from standard Beer's law curves for *p*-nitrotoluene.

Calculations and Treatment of Data—Figure 2 describes a simple semi-infinite sink model which assumes constant stirring in the aqueous phase resulting in a diffusion layer region. This region is effectively stagnant, and a quasi-steady-state constant hydrodynamic condition is assumed to exist in it. At the intestine-water interface, a concentration-independent partition coefficient, *K*, exists at equilibrium. In this model it can be assumed that the diffusion coefficient of the solute in the aqueous diffusion layer is *D_w*. The following equation describes the situation:

$$\frac{dC_w}{dt} = -\frac{D_w A}{hV_w}(C_w - C_I) \quad (\text{Eq. 1})$$

where *C_w* is the bulk solute concentration at any time *t*, *C_I* is the solute concentration at the intestinal mucosa at any time *t*, *D_w* is the aqueous solute diffusion coefficient, *A* is the total surface area of exposed mucosal surface, *h* is the diffusion layer thickness, and *V_w* is the aqueous bulk volume.

It is assumed that steady state is achieved early in the experiments and that the data obtained are employed in the calculation and treatment of the results. It is also assumed that during the experiments the intestine is still viable. This is supported by comparable experiments on the transport properties of rabbit intestines showing viability for periods longer than 1 hr (9). If this is so, then

¹ Radiochemical Center, Amersham, Buckinghamshire, England.

² New England Nuclear, Boston, Mass.

³ Nutritional Biochemicals Corp., Cleveland, Ohio.

⁴ Motor Division, Hurst Manufacturing Corp., Princeton, Ind.

⁵ Packard Tri-Carb model 3320, Packard Instrument Co., Downers Grove, Ill.

⁶ Perkin-Elmer model 202, Perkin-Elmer Corp., Norwalk, Conn.

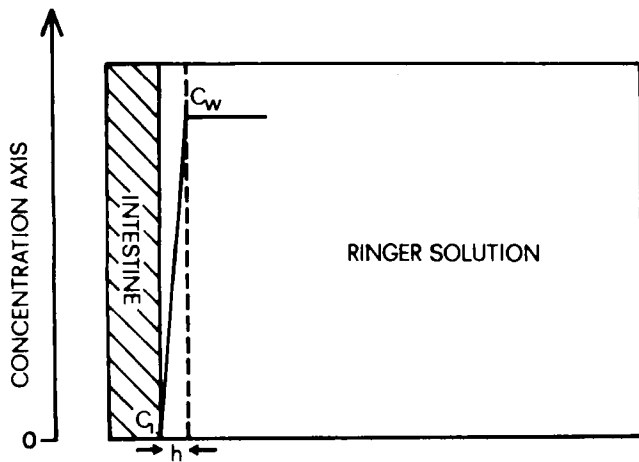


Figure 2—Simple semi-infinite sink model of solute transport across an aqueous diffusion layer of thickness h into the mucosa. C_w is the aqueous bulk concentration; C_1 is the interfacial (Ringer's solution–mucosal) aqueous concentration. The solid line in the Ringer's solution and aqueous diffusion layer represents condition at time equals zero.

Eq. 1 can be written as:

$$\frac{dC_w}{dt} = -\frac{D_w A}{h V_w} C_w \quad (\text{Eq. 2})$$

After separating the variables and integrating, one can obtain:

$$\ln C_w = -\frac{D_w A}{h V_w} t + \text{constant} \quad (\text{Eq. 3})$$

A plot of C_w versus t on semilogarithmic graph paper yields a straight line whose slope ($-D_w A/h V_w$) is the uptake rate constant. Since the calculated value is the initial slope, the constant isolated is designated as the initial uptake rate constant. Furthermore, when the partition coefficient K of the solute between the intestinal mucosa and the aqueous bulk phase is relatively large, the data are expected to deviate from linearity and Eq. 3 only applies for the first few initial points.

The diffusion layer thickness is calculated from the results obtained when p -nitrotoluene is used as the solute in Ringer's solution. The aqueous diffusion coefficient of p -nitrotoluene is reported to be about $1.1 \times 10^{-6} \text{ cm}^2/\text{sec}$ (8). Figure 3 is a semilogarithmic plot of p -nitrotoluene concentration remaining in the diffusion medium versus time in minutes. The best straight line joining the data points is drawn. When equating the slope to $-(D_w A/h V_w)$, substituting for $D_w = 1.1 \times 10^{-6} \text{ cm}^2/\text{sec}$, $V_w = 175 \text{ ml}$, and $A = 1.61 \text{ cm}^2$, and changing the slope from minute^{-1} to second^{-1} , the value of h was found to be 0.00046 cm .

For the uptake of cholesterol, the slopes of the lines from the semilogarithmically plotted data are equated to $-(D_w A/h V_w)$. The values of A , h , and V_w are also known; D_w for cholesterol is calculated in the different sodium cholate systems. The permeability coefficient, $P = (D_w/h)$, is also calculated.

Figure 4 reports the results on the determination of the CMC of sodium cholate in water and in Ringer's solution. The semilogarithmic plot of the number of droplets delivered per 5-ml volume at constant rate versus cholate concentration in mM resulted in

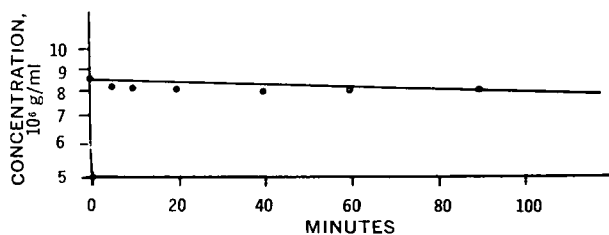


Figure 3—Semilogarithmic plot of p -nitrotoluene concentration remaining in the diffusion medium versus time in minutes.

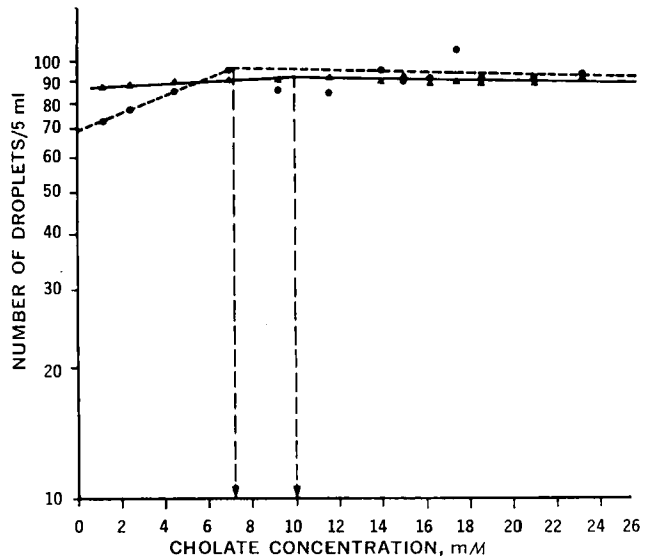


Figure 4—Semilogarithmic plot of number of droplets/5 ml versus cholate concentration in mM. Key: ●, data points when cholate is dissolved in water (the CMC determined is indicated with an arrow on the concentration axis and is 7.2 mM); and ▲, data points when cholate is dissolved in Ringer's solution (the CMC determined is indicated with an arrow on the concentration axis and is 10 mM).

points that could be linearly joined by two separate lines. One line joins the low cholate concentration data, and the other line joins the higher concentration data. The two lines intercept each other at the CMC as shown in the figure. The CMC of the cholate–water system is around 7.2 mM, while that of the cholate–Ringer's solution system is around 10 mM. These results agree with data reported previously (10).

RESULTS

Uptake of Cholesterol-4-¹⁴C Utilizing a Water-Jacketed Beaker of $V_w = 370 \text{ ml}$ —Experiments were run utilizing the same amount of cholesterol in Ringer's solution but altering the cholate concentration (pH of all cholate solutions studied ranged between 6.9 and 7.3). Figure 5 shows a representative plot of cholesterol (in counts/10 min) remaining in solution versus time in minutes. Each point in the graph represents at least three experimental runs. At 1.16, 2.32, and 4.64 mM cholate concentrations,

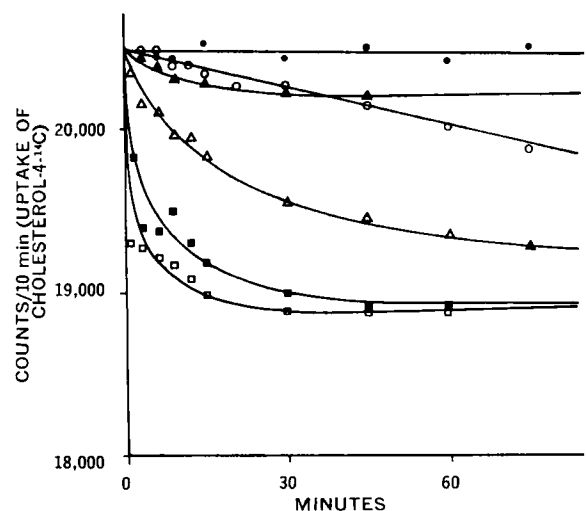


Figure 5—Plot of cholesterol-4-¹⁴C in counts/10 min left over in solution versus time in minutes when $V_w = 370 \text{ ml}$. Key: ○, 0 mM sodium cholate; △, 1.16 mM sodium cholate; ■, 2.32 mM sodium cholate; □, 4.64 mM sodium cholate; ▲, 11.16 mM sodium cholate; and ●, 17.40 mM sodium cholate.

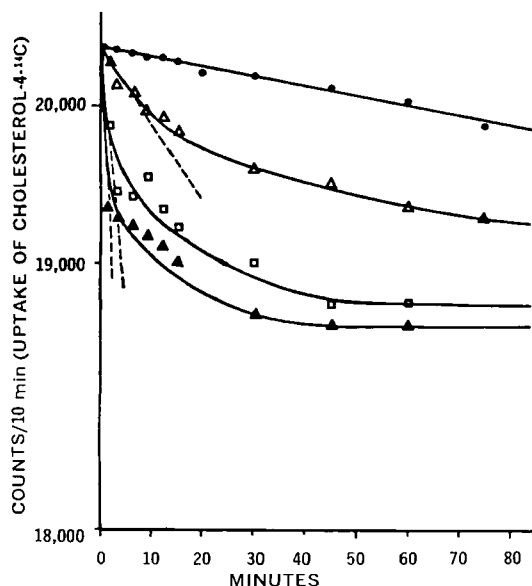


Figure 6—Semilogarithmic plot of cholesterol-4-¹⁴C in counts/10 min left over in solution versus time in minutes when $V_w = 370$ ml for some representative experiments. Key: ●, 0 mM sodium cholate; △, 1.16 mM sodium cholate; □, 2.32 mM sodium cholate; and ▲, 4.64 mM sodium cholate. The dotted lines are those joining the early experimental data points. The slopes of these lines were employed in the treatment of data.

there was an increase in the rate of cholesterol uptake as compared to the rate at 0 mM cholate concentration. This increase continued even at 6.38, 8.12, and 11.16 mM cholate concentration (Table I). The latter rates represent a decreasing trend when compared to those of 1.16, 2.32, and 4.64 mM levels of cholate. At 17.4 mM cholate, there seemed to be little or no uptake of cholesterol for 75 min.

Figure 6 represents a semilogarithmic plot of the concentration of cholesterol versus time for the 0, 1.16, 2.32, and 4.64 mM levels of cholate. The dotted lines are extensions of the straight lines passing through the early data points. The slopes of these lines and similar lines for the 6.38, 8.12, 11.16, and 17.40 mM levels were calculated and are reported in Table I. As indicated in the table there

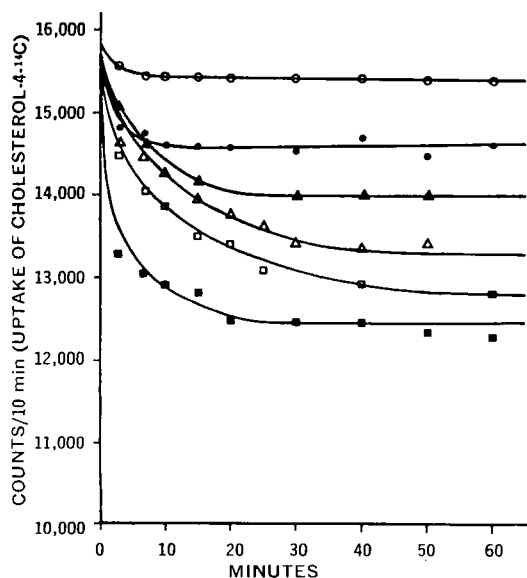


Figure 7—Plot of cholesterol-4-¹⁴C in counts/10 min left over in solution versus time in minutes when $V_w = 175$ ml. Key: △, 0 mM sodium cholate; □, 1.16 mM sodium cholate; ●, 2.32 mM sodium cholate; ●, 8.12 mM sodium cholate; ▲, 17.40 mM sodium cholate; and ○, 23.20 mM sodium cholate.

Table I—Estimated Initial Rates and Relative Initial Rates of Cholesterol Uptake into Rabbit Intestine as a Function of Cholate Concentration

Cholate in Ringer's Solution, mM	pH	Initial Rate Constant ^a , hr ⁻¹	Relative Initial Rate Constant ^b
0.00	6.90	0.024	1.00
1.16	6.92	0.166	6.90
2.32	7.00	0.976	40.70
4.64	7.00	4.560	190.00
8.12	7.05	0.244	10.17
11.16	7.15	0.059	2.50
17.40	7.30	0.000	0.00

^a Calculated from the slope of the line from the semilogarithmic plot passing through the first few experimental data points. ^b Calculated by dividing the initial rate of the system containing sodium cholate by the initial rate of the system containing 0 mM cholate.

was an increase in the relative initial rate constant as a function of cholate concentration, with a maximum being reached roughly around 4.64 mM of cholate. Below and above this cholate concentration, the relative initial rate constants showed a decline as compared to the maximum value.

Uptake of Cholesterol-4-¹⁴C Utilizing a Water-Jacketed Beaker of $V_w = 175$ ml—Figures 7 and 8 are representative plots of the uptake of cholesterol in Ringer's solution with different cholate concentrations. Both plots are similar to Figs. 5 and 6. The differences are indicated in the initial rate constants and not in their relative values. This is expected due to the differences in the diffusion layer thicknesses.

Uptake of Cholic-³H Acid Utilizing a Water-Jacketed Beaker of $V_w = 175$ ml—There was no significant cholic acid uptake by the rabbit intestine. This was observed in all cholate concentrations.

DISCUSSION

A novelty of such experiments resides in finding the effect of

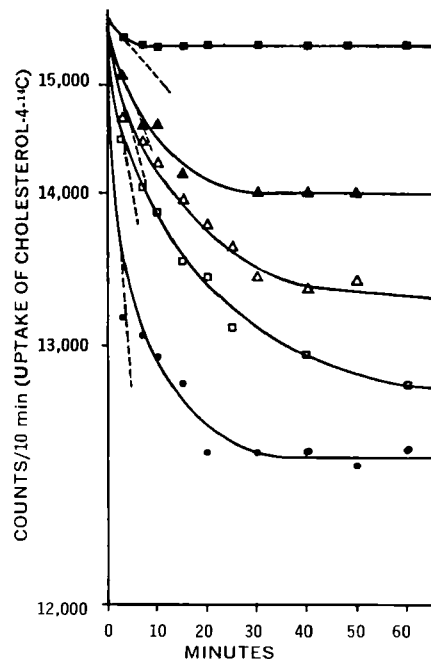


Figure 8—Semilogarithmic plot of cholesterol-4-¹⁴C in counts/10 min left over in solution versus time in minutes when $V_w = 370$ ml for some representative experiments. Key: △, 0 mM sodium cholate; □, 1.16 mM sodium cholate; ●, 2.32 mM sodium cholate; ▲, 17.40 mM sodium cholate; and ■, 23.20 mM sodium cholate. The dotted lines are those joining the early experimental data points. The slopes of these lines were employed in the treatment of data.

Table II—Estimated Diffusion and Permeability Coefficients of Cholesterol Uptake into Rabbit Intestine as a Function of Cholate Concentration

Cholate in Ringer's Solution, mM	Initial Rate Constant, hr ⁻¹	Diffusion Coefficient, cm ² /sec	Permeability Coefficient, cm/sec
0.00	0.928	1.30×10^{-5}	3.0×10^{-2}
1.16	1.499	2.10×10^{-5}	4.5×10^{-2}
2.32	2.929	4.10×10^{-5}	9.0×10^{-2}
8.12	1.392	1.90×10^{-5}	4.1×10^{-2}
17.40	0.644	9.00×10^{-6}	1.9×10^{-2}
23.20	0.260	3.60×10^{-6}	0.8×10^{-2}

some bile salt constituents on the transport of cholesterol by the intestinal epithelium. The question that could be raised here is whether cholate (one bile salt constituent) enhances cholesterol transport. Figure 5 and Table I clearly indicate that there is a substantial increase in the initial uptake rate of cholesterol across the intestinal barrier between the 1 and 10 mM cholate concentration range.

The CMC of sodium cholate in water was estimated to be in the range of 7.2 mM when determined by the volume-per-drop method, and the CMC of cholate in Ringer's solution was found to be around 10 mM (Fig. 4). Hofmann and Borgström (11) reported the CMC to be in the range of 20 mM of cholate when the latter acted as a solubilizing agent for 20-methylcholanthrene. With this in mind and considering the conditions of the intestinal content, it can be suggested that the CMC of cholate in the intestine is somewhere in the range of 10–20 mM. The data in Table I indicate that below the CMC the transport rate is fast and that close to the CMC the rate is declining; it is close to nil at around 18 mM when micelles are in existence.

Figures 7 and 8 further support the data. Because of the faster rate of transport of cholesterol in the $V_w = 175$ -ml beaker (compare the third column of Table I with the second column of Table II), it was easier to measure in it the diffusion layer thickness along the intestinal surface at a 120-rpm stirring rate. Table II presents the calculated diffusion coefficients of cholesterol in the different cholate solutions in Ringer's solution. Howard (8) reported the value of the diffusion coefficient, D_w , of cholesterol at 30° in water to be around 2.0×10^{-6} cm²/sec. From the Stokes-Einstein approximation, the calculated value of D_w of cholesterol was around 4.0×10^{-6} cm²/sec. In this study (Table II), the calculated diffusion coefficient of cholesterol in 0 mM cholate and at 37° was around 13.0×10^{-6} cm²/sec, which is in agreement with the reported data. As the cholate concentration increased, the value of the diffusion coefficient also increased. At higher cholate concentrations, there was a decrease in the D_w values; this decrease was maintained at and above the CMC of sodium cholate.

The calculated values of the permeability coefficients (Table II) agreed fairly well with the sequence of the results. There was roughly a 10 times decrease in the permeability coefficient value between the 2.32 and 23.2 mM cholate concentration levels. The differences obtained in the permeability coefficient values support the fact that this is a highly sensitive system. The values indicate that slight changes in the cholate concentrations showed significant changes in the permeability coefficients of cholesterol uptake.

The following explanation is given for the role that cholate plays on the uptake of cholesterol by the intestinal mucosa. The cholate-cholesterol interaction varies with the concentration of cholate in the system. Below the CMC, this interaction could be, for example,

nil, a 1:1 interaction, a 2:1 interaction, a 1:2 interaction, etc. Therefore, the concentration of free cholesterol in the medium is not altered drastically. This suggests that cholate may alter the permeability of the intestinal barrier (12) and, consequently, the effect of cholate at submicellar concentration levels. At or above the CMC, the formation of micelles yields stronger cholesterol-cholate interactions. The concentration of cholesterol in the micelles would be higher than in the aqueous surroundings, resulting in a higher partitioning tendency between the hydrophobic part of the micelle and its environment. Experiments with the cholic acid-cholate system ruled out the possibility that micelles are taken up by the mucosa for 1 hr. These experimental findings suggest that micelle formation retards cholesterol uptake by the mucosal surface of the intestine.

CONCLUSION

The data reported show that the uptake of cholesterol by the isolated rabbit intestine is enhanced in the presence of sodium cholate. The design of the apparatus and the geometry of the system made it possible to control the temperature, solute concentration, cholate concentration, and hydrodynamics. With these factors controlled, it was possible to determine quantitatively the initial rate constants, diffusion coefficients, and permeability coefficients of cholesterol during its passage across the mucosal surface of the rabbit intestine.

REFERENCES

- (1) E. B. Feldman and B. Borgström, *Biochim. Biophys. Acta*, **125**, 148(1966).
- (2) S. G. Schultz and C. K. Strecker, *Amer. J. Physiol.*, **220**, 59(1971).
- (3) C. Sylven and B. Borgström, *J. Lipid Res.*, **9**, 596(1968).
- (4) A. B. Bikhazi and W. I. Higuchi, *Biochim. Biophys. Acta*, **233**, 676(1971).
- (5) A. F. Hofmann, *Gastroenterology*, **48**, 484(1965).
- (6) J. Hajjar and P. F. Curran, *J. Gen. Physiol.*, **56**, 673(1970).
- (7) G. A. Bray, *Anal. Biochem.*, **1**, 279(1960).
- (8) S. A. Howard, Ph.D. dissertation, University of Michigan, Ann Arbor, Mich., 1968.
- (9) S. G. Schultz and R. Zalusky, *J. Gen. Physiol.*, **47**, 1043(1964).
- (10) A. B. Bikhazi and A. P. Simonelli, "Dissolution Rates of High Energy Sodium Cholate-Drug Coprecipitates," Abstract No. 68, presented to the Basic Pharmaceutics Section, APhA Academy of Pharmaceutical Sciences, San Francisco meeting, Mar. 1971.
- (11) A. F. Hofmann and B. Borgström, *Fed. Proc.*, **21**, 43(1962).
- (12) S. Feldman, M. Reinhard, and C. Wilson, *J. Pharm. Sci.*, **62**, 1961(1973).

ACKNOWLEDGMENTS AND ADDRESSES

Received November 28, 1973, from the *School of Pharmacy and the †Department of Physiology, School of Medicine, American University of Beirut, Beirut, Lebanon.

Accepted for publication May 6, 1974.

Presented to the Basic Pharmaceutics Section, APhA Academy of Pharmaceutical Sciences, San Diego meeting, November 11–15, 1973.

Supported in part by a grant from the University Medical Research Fund, American University of Beirut, Beirut, Lebanon.

* To whom inquiries should be directed.